

See discussions, stats, and author profiles for this publication at: <https://www.researchgate.net/publication/51171623>

# Performances of Mass-Sensitive Devices for Gas Sensing: Thickness Shear Mode and Surface Acoustic Wave Transducers

ARTICLE *in* ANALYTICAL CHEMISTRY · JULY 1996

Impact Factor: 5.64 · DOI: 10.1021/ac9600215 · Source: PubMed

---

CITATIONS

87

---

READS

11

5 AUTHORS, INCLUDING:



Andreas Hierlemann

ETH Zurich

290 PUBLICATIONS 4,834 CITATIONS

SEE PROFILE

# Performances of Mass-Sensitive Devices for Gas Sensing: Thickness Shear Mode and Surface Acoustic Wave Transducers

K. Bodenhöfer, A. Hierlemann,\* G. Noetzel, U. Weimar, and W. Göpel

*Institute of Physical and Theoretical Chemistry, Center of Interface Analysis and Sensors, University of Tübingen, Auf der Morgenstelle 8, D-72076 Tübingen, Germany*

**In this work we investigated different thickness shear mode resonators (TSMRs) with fundamental frequencies of 10 and 30 MHz and surface acoustic wave devices with fundamental frequencies of 80 and 433 MHz. Four aspects were of primary interest in this comparison: noise levels and signal-to-noise ratios (S/N), influence of the polymer film thickness, influence of temperature on the transducer signal before and after coating, and minimum threshold values for monitoring different volatile organic compounds in the environment. We limited our investigations to a temperature range between 298 and 308 K, with 303 K the routine measuring temperature. Analyte concentrations (*n*-octane, tetrachloroethene) were chosen from the minimum detection limit up to 5000 µg/L. The temperature was found to strongly affect the performance of all the devices. The sorption of the analyte vapors into the polymeric films was demonstrated to be transducer-independent (identical partition coefficients for all the devices). The 30 MHz TSMRs showed very satisfying results in terms of S/N and limits of detection.**

Mass-sensitive transducers are commonly used for monitoring gases and, in particular, for monitoring volatile organic compounds (VOCs) by using polymer layers as sensitive coatings. Two transducers are mainly utilized, i.e., thickness shear mode resonators (TSMRs) and surface acoustic wave (SAW) devices (see, e.g., refs 1–5). Since both kinds of transducers are directed at the same field of applications, a comparison of their properties and performances could be useful. The goal of this work was to evaluate the performances of the different devices with regard to practical applications in the field of environmental routine monitoring of hazardous compounds. In this context, the criteria included the following four aspects: noise levels and signal-to-noise ratios (S/N), influence of polymer film thickness, influence of temperature on the transducer signal before and after coating, and minimum threshold values for monitoring VOCs in the environment.

There exist fundamental differences in the physics of the transducer principles. Employing, e.g., thin Langmuir–Blodgett films<sup>6,7</sup> or self-assembled monolayers<sup>8,9</sup> as chemically sensitive

coatings, SAW devices offer clear advantages due to their high surface sensitivity.<sup>10</sup> On the other hand, they are more sensitive to small temperature fluctuations caused, e.g., by the carrier gas stream since the coating layers are thinner and the energies of these Rayleigh waves (propagating parallel to the surface) are confined to a zone at the surface approximately one acoustic wavelength thick.<sup>10</sup> The acoustic wavelength of the TSMRs, which is equivalent to twice the substrate thickness, is longer than that of the SAW; therefore, coatings on the TSMRs can be thicker (film thickness should be limited to 0.1–0.3% of the acoustic wavelength). In addition, the acoustic shear waves are propagating perpendicular to the surfaces. Thermal fluctuations are therefore expected to have less influence on the sensor's performance.

As shown by Sauerbrey<sup>11</sup> for TSMRs and by Wohltjen correspondingly for SAWs,<sup>2</sup> the vibrating frequency,  $f$ , of a quartz crystal changes to a first approximation proportionally to the mass deposited onto or removed from the surface:

$$\Delta f = -C f_0^2 \Delta m / A \quad (1)$$

where  $\Delta f$  is the frequency shift due to the added mass in hertz,  $C$  is a constant,  $f_0$  is the fundamental frequency of the quartz crystal in hertz, and  $\Delta m / A$  the surface mass loading in grams per square centimeter. After Ricco et al.,<sup>12</sup> the changes of the SAW frequency may formally be expressed as a sum of independent (the different derivatives of the frequency with respect to one variable are taken at constant other variables) contributions:

$$\Delta f = \frac{\partial f}{\partial m} \Delta m + \frac{\partial f}{\partial c} \Delta c + \frac{\partial f}{\partial \epsilon} \Delta \epsilon + \frac{\partial f}{\partial \sigma} \Delta \sigma + \frac{\partial f}{\partial T} \Delta T + \frac{\partial f}{\partial p} \Delta p + \dots \quad (2)$$

Here  $m$  denotes the mass,  $c$  the stiffness,  $\epsilon$  the dielectric constant,  $\sigma$  the conductivity,  $T$  the temperature, and  $p$  the pressure. Under

- (1) Snow, A. W.; Wohltjen, H. *Anal. Chem.* **1984**, *56*, 1411–1416.
- (2) Ballantine, D. S.; Wohltjen, H. *Anal. Chem.* **1989**, *61*, 705–712.
- (3) Grate, J. W.; Martin, S. J.; White, R. M. *Anal. Chem.* **1993**, *65*, 940A–948A; 987A–996A.
- (4) Amati, D.; Arn, D.; Blom, N.; Ehrat, M.; Sauniois, J.; Widmer, H. M. *Sens. Actuators B* **1992**, *7*, 587–591.
- (5) Nieuwenhuizen, M. S.; Venema, A. *Sens. Mater.* **1989**, *5*, 261–300.

- (6) Wohltjen, H.; Snow, A. W.; Barger, W.; Ballantine, D. S. *IEEE Trans. Ultrason., Ferroelectrics Freq. Contr.* **1987**, *UFFC-34*, 172.
- (7) Rapp, M.; Binz, D.; Kabbe, I.; von Schickfus, M.; Hunklinger, S. *Sens. Actuators B* **1991**, *4*, 103–108.
- (8) Kepley, L. J.; Crooks, R. M.; Ricco, A. J. *Anal. Chem.* **1992**, *64*, 3191–3193.
- (9) Sun, L.; Crooks, R. M.; Ricco, A. J. *Langmuir* **1993**, *9*, 1775–1780.
- (10) Wohltjen, H. *Sens. Actuators* **1984**, *5*, 307–325.
- (11) Sauerbrey, G. *Z. Phys.* **1959**, *155*, 206–222.
- (12) Ricco, A. J.; Martin, S. J.; Zipperian, T. E. *Sens. Actuators* **1985**, *8*, 319–333.

normal operating conditions (with  $T$  and  $p$  constant), it has been assumed that the contributions from changes in stiffness, dielectric constant, and relative permittivity are negligible in comparison to the effect of changes in surface mass. However, in recent publications,<sup>13–15</sup> this simple model was improved and, in particular, the general dominance of mass loading effects in SAW responses was questioned. The TSMR has the principal advantage of negligible influences from conductivity and permittivity (broad spectrum of applicable polymers). The acoustoelectric effect of quartz, used as substrate for both SAW and TSM devices, is sufficiently small that it is not worth mentioning, especially for the polymer films considered here.<sup>12</sup> The influence from stiffness on the TSMR response is smaller because of the lower operating frequency. The effects of temperature and pressure may, in principle, be reduced for all AW devices by operating at constant  $T$  and  $p$  or by appropriate referencing.

The theoretical approaches mentioned above predict the sensor responses ( $\Delta f$ ) to be proportional to the fundamental frequency,  $f_0$ , by a power of 2 (eq 1).<sup>1,2,4</sup> The higher the fundamental frequency of the device, the larger the sensor response to be expected. Using devices with higher operating frequency, however, does not necessarily improve the sensor performance.<sup>16</sup> To compare the overall performances of SAW and TSM devices, the following study is based on the pragmatic approach of Lorber.<sup>17</sup> The most useful figure of merit to characterize the quality of a sensor is its signal-to-noise ratio ( $S/N$ ), which is related to three other features of merit: (a) the precision, expressed as percent relative standard deviation in subsequent concentration measurements; (b) the limit of detection (LOD), which is the concentration of the analyte corresponding to  $S/N = 3$ ; and (c) the partial sensitivity ( $S \approx d(\Delta f)/dc_{\text{gas}}$ ), which is the slope of the analytical calibration curve.<sup>17</sup>

In this study, we restricted our investigations to monitoring VOCs by using such polymeric films for which physisorption and bulk dissolution within the polymer volume are the predominant mechanisms.

Observing a linear relation between VOC concentrations and the frequency shifts in the experiments (partial pressures of the VOCs below 10% of the saturation vapor pressure at the respective temperature), one can calculate partition coefficients,  $K$ , from

$$K = c_{\text{polymer}}/c_{\text{gas}}, \quad \text{with}$$

$$K = \frac{\Delta f_{\text{gas}} [\text{Hz}] \rho_{\text{polymer}} [\text{g/mL}] R [\text{J/K mol}] T [\text{K}] \times 10^7}{\Delta f_{\text{polymer}} [\text{Hz}] M_{\text{gas}} [\text{g/mol}] p_{\text{gas}} \times 0.98 [\text{ppm Pa}]} \quad (3)$$

Here,  $\Delta f_{\text{gas}}$  and  $\Delta f_{\text{polymer}}$  denote the frequency shifts upon gas exposure and polymer coating,  $\rho$  the polymer density,  $R$  the molar gas constant,  $T$  the temperature,  $M_{\text{gas}}$  the molar mass of the analyte,  $p_{\text{gas}}$  the gas phase partial pressure of the analyte, and  $10^7$  a scaling factor. The assumption is made that the analyte vapor in the carrier gas stream behaves like an ideal gas; therefore, the gas phase pressure of the analyte is expressed in parts per million of pascals ( $n/V = p/RT$ ). The factor 0.98 in the denominator takes

into account the air pressure in our laboratory since the system is open. The scaling factor  $10^7$  results from translating the original equation in SI units into the present form.  $K$  is dimensionless. The polymer volume in a first-order approximation is assumed not to be changed during the sorption of the analyte gas. Ideally, the experimentally determined partition coefficient should be constant for the chosen analyte/polymer combination and independent of the mass-sensitive transducer principle.

For comparative studies, the following two principal difficulties concern the adequate choice of suitable coatings.

**Polymer Properties.** We tried to select polymer coatings that make it possible to compare directly the sensor results obtained by different transducers. Consequently, only nonconducting polymers and polymers with low static glass transition temperatures were suitable. The apparent (high-frequency) glass transition temperature of the respective polymer may be 50–60 K higher than the static one usually known from literature. It depends strongly on the frequency of the acoustic wave.<sup>13,18</sup> Even the comparison of SAW devices operating at different frequencies may therefore not be straightforward. In this context, soft, rubbery polymer films are generally most suitable as they are highly permeable. Applying higher operating frequencies, the contributions included in the sensor signals of polymer properties like stiffness or shear modulus may change on going from the rubbery to the glassy state. Consequently, the influence of plasticization and softening effects on the sensor response may change as well.

**Layer Thickness.** The thickness of the polymer layers applied varied between 300–600 nm for 10 MHz TSMRs and 10–30 nm for 433 MHz SAWs. Generally, the coating thickness that can be applied without quenching oscillation will decrease as the device frequency is increased.<sup>1,16</sup> Wohltjen and Snow suggested as a guideline that coating thickness for SAWs should be in the range of 1% of the acoustic wavelength (for quartz substrates, 433 MHz, 73 nm; 80 MHz, 395 nm),<sup>1</sup> thus ignoring the polymer properties. Ricco<sup>19</sup> proposed as a limit of the layer thickness  $d \ll \lambda_0 (v_t/v_0)^2$ . Here,  $\lambda_0$  denotes the acoustic wavelength,  $v_t$  the velocity of acoustic shear waves in the polymer film, and  $v_0$  the SAW velocity (3.16 km/s for quartz). Suitable thickness for the comparisons made here, however, was determined by the experimental value of the partition coefficient  $K$ , which was calculated as described in eq 3. Within experimental error, the QMB generally is assumed to act as a nearly ideal gravimetric detector due to the low operating frequency. We obtained partition coefficients from QMB measurements with a standard deviation below 5% for different TSM devices and measurements. In exposing all the sensors only to low analyte concentrations (below 5000  $\mu\text{g/L}$ ), the effects of plasticization, film softening, swelling, etc., on the SAW response were reduced (in practical applications, there is an urgent need for monitoring trace level concentrations). Consequently, we were able to determine corresponding partition coefficients from TSMR and SAW measurements (e.g., log  $K$  tetrachloroethene/SE 30, 10 MHz, 3.21; 30 MHz, 3.19; 80 MHz, 3.25; 433 MHz, 3.20). We chose the values of these partition coefficients to determine the maximum layer thickness of the SAWs up to which mass loading effects still dominate. In this way, we tried to compare the

(13) Martin, S. J.; Frye, G. C.; Senturia, S. D. *Anal. Chem.* **1994**, *66*, 2201.

(14) Grate, J. W.; Snow, A. W.; Ballantine, D. S.; Wohltjen, H.; Abraham, M.; McGill, R. A.; Sasson, P. *Anal. Chem.* **1988**, *60*, 869–875.

(15) Stone, D. C.; Thompson, M. *Anal. Chem.* **1993**, *65*, 352–362.

(16) Grate, J. W.; Klusty, M. *Anal. Chem.* **1991**, *63*, 1719–1727.

(17) Lorber, A. *Anal. Chem.* **1986**, *58*, 1167–1172.

(18) Ballantine, D. S.; Wohltjen, H. In *Chemical Sensors and Microinstrumentation*; Murray, R. W., Dessy, R. E., Heineman, W. R., Janata, J., Seitz, W. R., Eds.; ACS Symposium Series 403; American Chemical Society: Washington, DC, 1989; Chapter 15, pp 222–235.

(19) Ricco, A. J. *Electrochem. Soc. Interface* **1994**, *3* (4), 38–44.

gravimetric responses and to exclude the influence of additional effects on our comparative study. There may be instances where other sensing mechanisms such as viscoelastic responses or acoustoelectric effects could be used to advantage to get a more sensitive or more selective sensor. On the other hand, in applying thick layers, film resonance effects may occur, and the velocity response may be multivalued: several concentrations lead to the same velocity change (problematic for any practical application),<sup>13</sup> and it will not be possible to predict the approximate size of the response for various possible film/analyte combinations, since it is not possible at present to predict the magnitude of viscoelastic interactions. If one wishes to use the vast literature that describes interactions between films and absorbed molecules to design the respective sensor in advance rather than being forced to collect empirical data for each film and analyte in order to deal with non-mass-related effects, it is crucial to stick with films and thicknesses that lead to dominating mass response.

The maximum layer thickness depends on the transducer design, the operating frequency of the device, the applied analyte concentrations, and the polymer nature. Martin et al.<sup>13</sup> designated films showing a linear response behavior controlled by absorption thermodynamics as "acoustically thin" films. As a rule of thumb, the upper limit for the thickness,  $d$ , of viscoelastic acoustically thin films was given as  $d \ll |G|/(\hbar \nu_0 \rho)$ ,<sup>13,19</sup> where  $G$  is the shear modulus of the polymer (for viscoelastic polymers, typically  $10^7$  N/m<sup>2</sup>),  $\rho$  the film density (for polysiloxanes, in the order of 1 g/mL),  $\hbar$  the oscillation frequency, and  $\nu_0$  the SAW velocity (3.16 km/s for quartz).

On the other hand, the polymeric films may not be so thin that coadsorption of analyte molecules may occur at the transducer surface and at the polymer substrate interface (details in the Results section). A closed polymer surface is required in order to achieve evaluable gas/polymer partitioning.

## EXPERIMENTAL SECTION

**Transducers and Instruments.** For TSM devices, the setup consisted of discrete piezoelectric quartz crystals (AT-cut) with gold electrodes and fundamental frequencies of 10 MHz (thickness of the quartz plate, 167  $\mu$ m) and 30 MHz (thickness, 55.6  $\mu$ m), purchased from Kristallverarbeitung Neckarbischofsheim, Germany. Each crystal was powered by an oscillator circuit (bipolar, parallel resonance) constructed in our laboratory. Only a single coaxial cable is required for voltage supply and signal transmission. A self-developed scanner operating at frequencies between 100 kHz and 100 MHz was controlled by a PCL 726 interface card (Labtech, Wilmington, DE) in an IBM-compatible PC-AT and allowed for the sequential monitoring of each TSMR output using a Hewlett-Packard 5334B frequency counter. For the SAWs, we employed a commercially available 80 MHz setup (dual delay lines, quartz, aluminum electrodes, ST-cut, acoustic wavelength 39.5  $\mu$ m; Xensor Integration, Delft, The Netherlands<sup>20</sup>) and 433 MHz resonators (R 2632, Siemens, two discrete devices, quartz, aluminum electrodes, ST-cut, acoustic wavelength 7.3  $\mu$ m) with a circuitry (applicable up to 1.2 GHz) developed at the University of Heidelberg.<sup>21</sup> Both sensing units have three individual outputs, two for the reference and sensing line and a third for the mixer (difference frequency) output. The SAW outputs were directly

connected to the frequency counter inputs. The computer acquired the frequency values via an IEEE 488 interface bus. The first monitored frequency value of each device was set equal to zero, and the frequency differences were monitored in reference to this first value.<sup>22</sup>

The frequency outputs of the TSMRs and the mixers were recorded every 30 s at 0.1 Hz resolution, along with the individual line frequencies of the 80 MHz SAW. The 433 MHz individual line outputs were collected during vapor testing at 1 Hz resolution. The gate time of the counter (HP 5334 B) was set to 1 s for all transducers tested. The sensor responses are given by the frequency difference between gas exposure and purging.

**Sensor Coatings.** As described in the introduction, certain boundary conditions restrict the selection of those polymer coatings, which makes it possible to compare directly the sensor results obtained by different transducers: only nonconducting polymers and polymers with low static glass transition temperatures are suitable. Delay line structures may be coated only at the surface between the SAW launching and detecting interdigital transducers (IDTs), and these consequently allow for the use of conducting polymers. It has, however, to be noted that the Wohltjen equation has to be modified with respect to the relative coverage of the device active area.<sup>23</sup> Since in our case resonator structures should be included in the comparison, the finger electrodes generally were coated as well. The TSM devices were coated on both sides.

The following coatings (Figure 1) were finally chosen: poly(dimethylsiloxane) (SE 30, Macherey & Nagel, Düren, Germany), poly(cyanopropylmethylsiloxane) (PCPMS, Hüls Petrarch, Bristol, PA), and poly(ether urethane) (PEUT, Thermedics Inc., Woburn, MA). The polysiloxanes were found to be extremely long-term stable, as reported earlier,<sup>22</sup> and exhibit low static glass transition temperatures around 150 K. Although dynamic transition temperatures are higher than the static ones, we assume even for the 433 MHz SAWs the measuring temperature of  $T = 303$  K to be below this transition.

For film preparation, the polymers were dissolved in dichloromethane (concentrations of 1 mg/mL). The solutions were sprayed onto the cleaned devices (coating of the entire line including the electrodes) with an airbrush using pure nitrogen as carrier gas. On-line monitoring of the frequency decrease allowed determination of the frequency shifts due to coating. The layer thickness ( $d$ ) then was calculated, assuming a uniform and homogeneous distribution of the polymer over the sensitive surface. REM and AFM shots of the films showed that this assumption is reasonable for nonpolar polymers. Polar polymers may lead to droplets since the cohesion forces within the polymer molecules are stronger than the adhesion at the quartz or gold surface.

In the first step, we used layers as thick as possible up to the limit where the acoustic wave was quenched by damping and phase shift. This maximum thickness was strongly dependent on polymer properties like stiffness, shear modulus, etc. The frequency shifts due to coating amounted to, e.g., for SE 30, 12–15 kHz ( $d = 440$ – $670$  nm) for the 10 MHz and 40–65 kHz ( $d = 180$ – $320$  nm) for the 30 MHz TSM devices. For the 80 MHz dual delay lines, the largest frequency decrease achievable (SE 30)

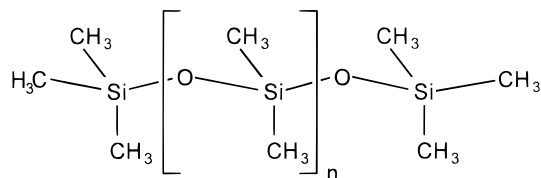
(20) Nieuwenhuizen, M.; Nederlof, A.; Vellekoop, M.; Venema, A. *Sens. Actuators* **1989**, *19*, 385–392.

(21) von Schickfus, M.; Stanzel, R.; Kammereck, T.; Weiskat, T.; Dittrich, W.; Fuchs, W. *Sens. Actuators B* **1994**, *18–19*, 443–447.

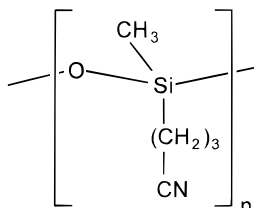
(22) Hierlemann, A.; Kraus, G.; Weimar, U.; Göpel, W. *Sens. Actuators* **1995**, *26*, 126–134.

(23) Ricco, A. J.; Martin, S. J. *Thin Solid Films* **1991**, *206*, 94–101.

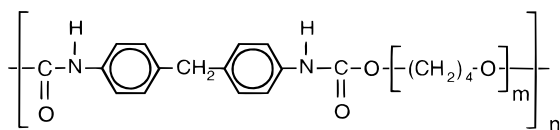
# Polymers:



Polydimethylsiloxane (SE 30)



Poly(cyanopropyl)methylsiloxane (PCPMS)



Poly(etherurethane) (PEUT)

Figure 1. Polymers used for coating the AW devices.

was about 1.2 MHz ( $d = 1560$  nm), and for the 433 MHz SAW it was about 650 kHz ( $d = 30$  nm). For the TSMRs in parallel resonance, we could use layers up to this maximum thickness since the partition coefficient was constant. In this case, the performance of the circuitry was the thickness-limiting factor. As described in the introduction, the layer thickness of the SAWs then was restricted to the range of predominantly gravimetric (linear) response using the thickness-independent partition coefficient as a criterion ( $\pm 10\%$  deviation).

The thicknesses of PCPMS layers on SAW devices were smaller because of the low but not negligible conductivity ( $0.1\text{--}0.5\ \mu\text{S}$  at 10 kHz), although PCPMS is usually considered to be a "nonconducting" polymer. The conductivity is likely to be ionic, not electronic, in nature and may result from ionic impurities.

**Gas Mixing.** The test vapors were generated from cooled ( $T = 243\text{--}263$  K) bubblers using synthetic air as carrier gas and then diluted to known concentrations by the computer-driven mass flow controllers. The vapor phase concentrations at the respective temperatures were calculated following the Antoine equation. All vapors were mixed and temperature stabilized before entering the thermoregulated chamber. The thermostat used was a microprocessor-controlled Julabo FP 30 MH (Julabo, Seelbach, Germany; precision of 0.01 K guaranteed). A temperature monitoring quartz resonator within the chamber (33.9 MHz, 90 ppm/K; KVG, Neckarbischofsheim, Germany) allowed us to determine the temperature fluctuations at 0.0005 K resolution. The gas flow rate was 200 mL/min at a total pressure of  $10^5$  Pa. The response time of the sensors is in the order of seconds ( $< 2$  s). However, the time necessary to reach an equilibrium state in our setup is about 10 min ( $t_{90} = 6$  min) and results from adjusting a constant gas

Table 1. Thermal Behavior and Sensor Responses of the Different Transducers and Coatings (for Details, See Text)

device	coating	$\Delta f_{\text{poly}}$ (kHz)	$\Delta f/\Delta T$ (Hz/K) <sup>a</sup>	$\Delta f_{\text{gas}}$ (Hz) 680 $\mu\text{g/L}$ , (100 ppm) per	$\left  \frac{\Delta f_{\text{gas}}}{\Delta f/\Delta T} \right $ (K)
TSMR					
10 MHz	uncoated		-3		
	SE 30	-9.2	-0.5	10.2	20
	PEUT	-11.6	-0.7	14.8	21
	PCPMS	-11.0	+1.5	6.2	4
30 MHz	uncoated		+5		
	SE 30	-48.1	-13	51.1	4
	PEUT	-71.6	-15	82.5	5.5
	PCPMS	-64.2	+25	32.5	1.3
SAW					
80 MHz	uncoated		+120 sl +180 mo		
	SE 30	-1150	-2750 sl +2800 mo	1420	0.5
	PEUT	-330	-160 sl +260 mo	304	1.9
	uncoated		-240 sl -270 mo		
433 MHz	SE 30	-443	-600 sl +480 mo	454	0.8
	PEUT	-190	-650 sl +550 mo	254	0.4

<sup>a</sup> sl, single line; mo, mixer output.

concentration in the chamber at the chosen flow rate. Typical experiments consisted of alternating exposures to air and vapor. Exposure times of 30 min were followed by 30 min of purging the chamber with synthetic air.

## RESULTS AND DISCUSSION

**Temperature Effects.** In the first part of our study, we investigated the shifts of the vibrational frequencies upon temperature changes. In ST-cut quartzes (mainly used for SAWs), for example, the velocity varies parabolically with temperature, with a turnover temperature of 293 K. We monitored only the resonance frequencies (and hence the velocity, not the attenuation, responses) by using a frequency counter. We always tested 5–10 devices as representatives for the respective kind of AW sensor.

We first investigated the temperature behavior of the *uncoated devices* between 298 and 308 K. The results for the different uncoated devices of the same type were very consistent ( $\sim 10\%$  deviation). We therefore list an average value in Table 1.

We then studied the additional temperature effects of the polymer layers on the *coated devices*. For this purpose, we prepared in the same run three or four devices with comparable layer thicknesses (i.e., frequency shift  $\Delta f_{\text{poly}}$ ) for each polymer.

Last we tried to evaluate the contribution of the *circuitry* to the temperature behavior. We stabilized the circuitry at the same temperature as the devices in one experiment; in another we thermally isolated the circuitry and kept it at 298 K while ramping the temperature of the devices.

For the SAWs, we recorded the individual as well as the mixer outputs to estimate whether or not thermal influences can be suppressed by referencing. As can be seen from Figure 2, even the sign of the temperature drift depends on the polymer employed, and, in particular, SE 30 and PCPMS (both polysiloxanes) show reproducibly contrasting behavior. Reasons for this effect result from the film morphology (PCPMS is a polar polymer,

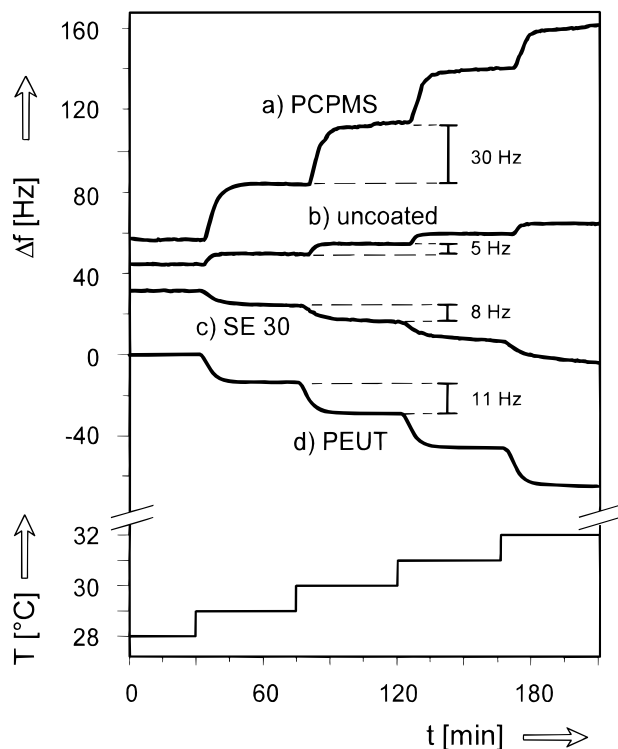


Figure 2. Temperature effects on a 30 MHz TSM device.

and we observed the formation of droplets rather than a closed film) and changes in the intrinsic polymer properties (shear modulus and thermal expansion). The signs of the temperature shifts for the respective coating generally are identical for all transducers operating between 10 and 433 MHz.

The coating-induced frequency shifts add vectorially to the values of the bare transducer. Sometimes, then, a compensation of the temperature effects of bare device and polymer may lead to minor temperature drifts of the coated devices, e.g., 30 MHz TSMRs and 80 MHz SAWs. Typical experimental data for SE 30 and PEUT are listed in Table 1. The values in columns 3 (frequency shifts due to coating) and 4 (frequency shift per K,  $\Delta f/\Delta T$ ) are device-specific. They differ for the respective coatings, layer thicknesses, and transducers.

We tried to prepare a set of comparable sensors for each type of transducer, but the discrepancies were somewhat significant. So we selected for the comparison of transducers in Table 1 those devices showing the "majority behavior" in our test sets. In our opinion, it is, however, always necessary to calibrate each single-coated AW device with respect to thermal effects, which following our observations mainly depend on the film morphology. Even devices coated with films of equal thickness (identical  $\Delta f$ ) using the same polymer solution on the same day may differ significantly in their thermal behaviors.

The fourth column of Table 1 gives the ratio of the sensor responses,  $\Delta f_{\text{gas}}$ , on exposure to 680  $\mu\text{g/L}$  (100 ppm) of tetrachloroethene (per) to the frequency shift by a temperature change of 1 K. These ratios do not depend on the layer thickness, as they are determined from the ratio of two thickness-dependent quantities. The dependence of the temperature effects on the polymer layer thickness is shown in Figure 3. There is a clear increase in the temperature drift on applying thicker layers. The "induction behavior" at the beginning may be a consequence of a too thin, nonclosed polymer layer (compare Figure 8). The data were

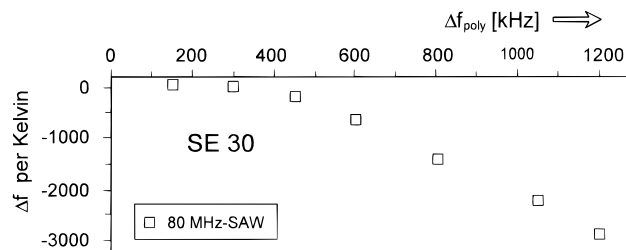


Figure 3. Frequency shift by temperature change of 1 K versus increasing polymer layer thickness (represented by  $\Delta f_{\text{poly}}$ ) of SE 30 on a 80 MHz SAW device.

collected as single line outputs, and the temperature drift of the bare device was subtracted.

The data in the fourth column were obtained by averaging over several measurements. They therefore characterize the temperature stability of the sensors and constitute a measure for the capability of each transducer to operate under real environmental conditions. It is evident that the TSMRs are less sensitive to temperature changes than SAWs. The signals from the mixer outputs of the SAWs are not directly useful in characterizing the thermal behavior. Nevertheless, we listed these data and showed them in the figures to illustrate that the dominant temperature-induced effects result from the coatings and not from the transducers. Consequently, any referencing of sensor signals may be useful to avoid the readout of high frequencies with high-speed counters but is not useful to compensate thermal effects. Even if both SAW lines are on the same substrate, appropriate compensation or correction is impossible (see results of 80 MHz devices with dual delay lines in Figure 4). Similar observations were made by Liron et al.<sup>24</sup> using polyisobutylene layers on 104 MHz delay lines. The authors also found that the temperature-induced frequency shift function depended on the nature of the coating of the delay line surface. It changed from a flat parabolic function of uncoated quartz delay lines near room temperature to a steep, almost linear curve for polymer-coated delay lines in the same temperature range, the slope of the curves depending on the nature of the polymer.<sup>24</sup>

The influence of temperature, especially on the frequency of coated SAW devices, is pronounced. For all devices, the temperature effects induced by the coatings exceed by far the thermal drifts of the bare devices. To overcome this drift problem, the most useful approach may be to first measure the temperature-induced frequency functions of the complete sensors, to incorporate additionally excellent temperature sensors such as the 33 MHz TSMR described above, or SAW devices on  $\text{LiNbO}_3$  substrates<sup>25,26</sup> into the sensing array, and to suppress the temperature-induced contributions mathematically by applying the correction algorithms obtained in the calibration. Alternatively, new methods for SAW sensing, such as reflection techniques,<sup>27</sup> could be applied.

The last point was to investigate the contribution of the circuitry. We were not able to find a significant difference in the frequency shifts due to temperature between stabilizing the

(24) Liron, Z.; Greenblatt, J.; Frishman, G.; Gratziani, N.; Biran, A. *Sens. Actuators B* **1993**, 12, 115–122.

(25) Viens, M.; Cheeke, J. D. *Sens. Actuators A* **1990**, 24, 209–211.

(26) Neumeister, J.; Thum, R.; Lüder, E. *Sens. Actuators* **1990**, A21–A23, 670–672.

(27) Becker, H.; van Schickfus, M.; Hunklinger, S. *Proc. Transducers* **1995**, 2, 720–723 (419–D7).

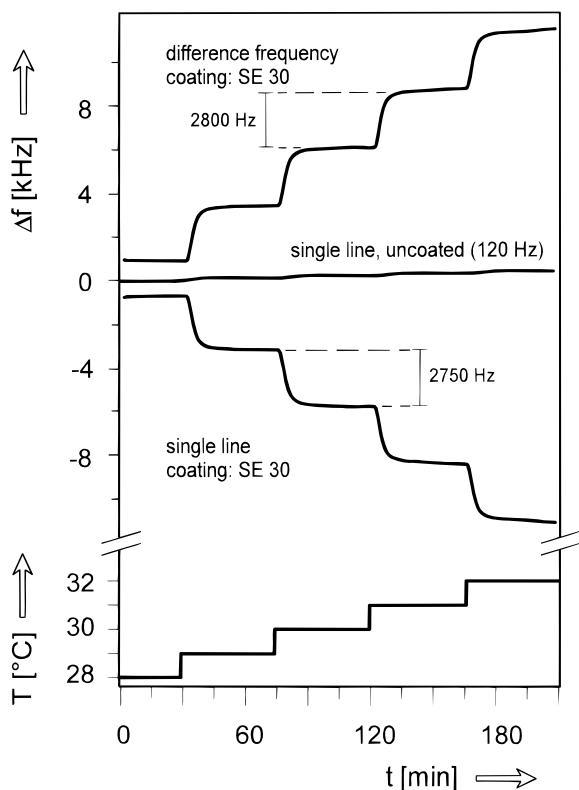


Figure 4. Frequency changes with temperature for the 80 MHz SAW dual delay line device (single line output).

circuitry at the same temperature as the devices and stabilizing it at 298 K. However, we found a pronounced increase in the frequency noise of all the devices if the circuitry was not at the same temperature as the sensor: for 10 MHz TSMRs from 0.01 to 0.1 Hz, for 30 MHz TSMRs from 0.03 to 0.15 Hz, for 80 MHz SAWs from 1.5 to 2.5 Hz, and for 433 MHz SAWs from 4 to 8 Hz.

Keeping the device and the circuitry at the same temperature consequently is crucial to reduce the frequency noise.

**Gas Tests.** We restricted our investigations to analyte concentration ranges (0–5000  $\mu\text{g/L}$ ) where the responses of all the devices were linearly (maximum deviation of 3%) dependent on the vapor concentration. The urgent need for sensors to detect organic pollutants at trace level justifies this restriction. Exposing the sensors to higher concentrations generally (all kinds of polysiloxanes, cellulose derivatives, etc.) leads to nonlinearities in the sensor responses, as demonstrated for poly(ether urethane) and *n*-octane in Figure 5, since Henry's law is no longer valid. The response and equilibrium times increase. It is no longer possible to calculate unequivocal partition coefficients. The deviations from linear behavior are reproducible using different kinds of devices or transduction principles (SAW, TSMR, capacitors, switched capacitors) and depend strongly on the nature of the analyte vapor and the respective polymer. Since the capacitors, which do not operate at high frequencies, show the same behavior, it cannot be a modulus effect. Similar behavior has been observed by other authors investigating the sorption of various gases in polyethylene by using a balance.<sup>28,29</sup> The authors describe such bent (toward higher sorption coefficients) curves as typical of sorption behavior in rubbery polymers.<sup>29</sup>

In our experimental setup, we measured all the devices simultaneously. In a first approach, we thus determined the

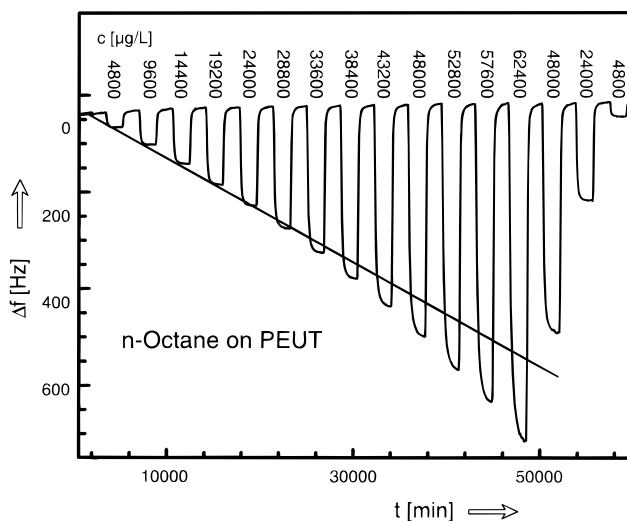


Figure 5. Nonlinearities in the sensor response occurring for higher gas phase concentrations, e.g., 10 MHz TSMR, *n*-octane on PEUT.

concentrations of vapors absorbed into the polymer films by assuming that the 10 MHz TSMRs respond as ideal gravimetric detectors. This control was important since the SAW velocity may decrease in some regimes of gas phase concentrations while increasing in others,<sup>13</sup> thus leading to ambiguous results. Such effects arise from polymer plasticization or vapor-induced softening.<sup>14,30</sup> In evaluating our signals, however, we got nearly identical (within experimental error) results upon calculating partition coefficients from SAW and TSMR measurements at low analyte concentrations. So, we were able to limit the film thickness as described in the introduction and experimental part by using the partition coefficient as a criterion.

From the identical partition coefficients for all the AW devices, we conclude that the mechanisms, i.e., mass loading (dominant) and viscoelastic effects, occurring at low analyte concentrations are similar for all AW devices coated with thin layers. Prior studies<sup>13,31</sup> have shown that both devices demonstrated a sensitivity to viscoelastic and film resonance effects if the films were sufficiently thick and had the appropriate modulus. Grate et al. described the predominant role of swelling-induced modulus changes of the polymers in determining the SAW responses.<sup>30</sup> A computer modeling of influences of changes in thickness, density, and stiffness on SAW responses is given in ref 32 for different polymers at various film thickness. Here, for thin layers, the SAW response is, according to the authors, less affected by changes of elastic stiffness.<sup>32</sup>

Therefore, the swelling and thermal expansion coefficients were experimentally determined by reflectometric interference spectrometry (RIFS) and ellipsometry<sup>33</sup> by G. Kraus and co-workers at our institute. For tetrachloroethene, e.g., the relative swelling coefficient (optical layer thickness) of SE 30 was  $1.06 \times 10^{-6}$  per  $\mu\text{g/L}$  gas phase concentration, and that for PEUT was  $1.44 \times 10^{-6}$  per  $\mu\text{g/L}$ .<sup>34</sup> The thermal expansion coefficients determined by

(30) Grate, J. W.; Klusty, M.; McGill, R. A.; Abraham, M.; Whiting, G.; Andonian-Haftvan, J. *Anal. Chem.* **1992**, *64*, 610–625.

(31) Martin, S. J.; Frye, G. C. *Proc. IEEE Ultrason. Symp.* **1991**, 393.

(32) Zellers, E. T.; White, R. M.; Wenzel, S. W. *Sens. Actuators* **1988**, *14*, 35–45.

(33) Gauglitz, G.; Brecht, A.; Kraus, G.; Nahm, W. *Sens. Actuators B* **1993**, *11*, 21–27.

(34) Kraus, G.; Klotz, A.; Seemann, J.; Spaeth, K.; Gauglitz, G. *Fresenius J. Anal. Chem.* **1995**, *352*, 426–430.

(28) Castro, E.; Gonzo, E.; Gottifredi, J. J. *Membr. Sci.* **1987**, *3*, 235–248.

(29) Doong, S.; Winston Ho, W. *Ind. Eng. Chem. Res.* **1991**, *30*, 1351–1361.

Table 2. Characteristic Data for the Different Transducers<sup>a</sup>

coating	device	noise (Hz)		$\Delta f_{\text{gas}}$ (Hz)	S/N	LOD ( $\mu\text{g/L}$ )	
		$\Delta f_{\text{poly}}$ (kHz)	bare device				coated device
Tetrachloroethene, 680 $\mu\text{g/L}$ (100 ppm)							
SE 30 (log $K = 3.20$ )	10 MHz	9	<0.1	<0.1	10.2	100	34
	30 MHz	48	<0.1	<0.1	51.1	500	7
	80 MHz	1150	0.3–0.5	3–5	1420	350	14
	433 MHz	440	0.5–1	3–5	454	115	21
PEUT (log $K = 3.25$ )	10 MHz	11.6	<0.1	<0.1	14.8	150	21
	30 MHz	71.6	<0.1	<0.1	82.5	800	7
	80 MHz	330	0.3–0.5	1–3	304	150	21
	433 MHz	190	0.5–1	1–3	254	130	21
<i>n</i> -Octane, 470 $\mu\text{g/L}$ (100 ppm)							
SE 30 (log $K = 3.35$ )	10 MHz	9	<0.1	<0.1	9.1	90	25
	30 MHz	48	<0.1	<0.1	44.2	440	10
	80 MHz	1150	0.3–0.5	3–5	1360	340	10
	433 MHz	440	0.5–1	3–5	305	75	35
PEUT (log $K = 2.80$ )	10 MHz	11.6	<0.1	<0.1	3.7	37	45
	30 MHz	71.6	<0.1	<0.1	20.6	200	15
	80 MHz	330	0.3–0.5	1–3	87.9	45	75
	433 MHz	190	0.5–1	1–3	changes in stiffness		

<sup>a</sup>  $\Delta f_{\text{poly}}$ , frequency shift due to coating, frequency noise (short time) for the bare and coated devices;  $\Delta f_{\text{gas}}$ , sensor responses to 470  $\mu\text{g/L}$  octane and 680  $\mu\text{g/L}$  tetrachloroethene; S/N, signal-to-noise ratio (the TSMR noise was set to 0.1 Hz for all the calculations); LOD, limit of detection (S/N = 3); log  $K$ , logarithm of the partition coefficient.

the same method were  $6 \times 10^{-4}/\text{K}$  for SE 30 and  $5 \times 10^{-4}/\text{K}$  for PEUT. For a maximum analyte gas phase concentration of 5000  $\mu\text{g/L}$ , the resulting relative increase of the layer thickness is 0.58% for SE 30 and 0.73% for PEUT. The relative swelling coefficient was found to be a constant for analyte vapor concentrations below 30 000  $\mu\text{g/L}$ . Applying high gas phase concentrations of the respective analytes leads to nonlinearities, as observed for the other devices. The swelling coefficients were dependent on the nature of the polymer as well as on the analyte (type of interaction mechanisms occurring) and were somewhat different from those calculated by adding the volumes of the polymer and the analyte in its liquid state.<sup>34,35</sup>

In our study, however, the observed sensor responses due to gas exposure and the calculated partition coefficients were lower than expected in assuming strong volume and modulus effects caused by swelling (according to ref 30).

Typical AW sensor data for the employed polymers (average values) are summarized in Table 2. The signals,  $\Delta f$ , obtained from SAW devices are evidently larger than those from TSMRs. On the other hand, the SAWs show larger noise levels. The 30 MHz TSMRs showed very favorable S/N and LOD values. The noise levels as well as the LOD values depend on the polymer nature and the layer thickness of the coatings. In our case, the frequency noise tended to increase with increasing layer thickness. At a first glance, it was surprising that the 30 MHz TSMRs were quite a bit better than the SAW devices in limit of detection. The thickness of the 30 MHz device was about 55  $\mu\text{m}$ . The acoustic wavelength for the 80 MHz SAW device was about 40  $\mu\text{m}$ . So, the energies of the 30 MHz TSMR and the 80 MHz SAW devices were concentrated in regions of very similar size. This means their sensitivities should be similar. The TSM device showed better performance because it was much less sensitive to the small

fluctuations in shear modulus (appearing as frequency noise) that occur in the polymer with small temperature changes.<sup>36</sup>

For SE 30-coated SAWs, e.g., the noise was correlated with the temperature fluctuations. This was proven by calculating the expected noise from the temperature fluctuations monitored separately with the quartz thermosensor ( $\Delta f = 8.9$  Hz, 33 MHz, 90 ppm/K). But generally it is not possible to simply say that the noise level is determined by similar temperature-induced fluctuations in polymer properties for all the different acoustic wave devices. One has to take care of possible changes in the polymer modulus (e.g., glass transitions), which strongly depend on the operating frequency.

The noise levels reported here were determined from sensor baseline frequency data during vapor response experiments as root mean square (RMS) values over a period of 10 min. These RMS values (uncoated and coated devices) are not the best achievable in a particular measurement but are averaged over a series of routine measurements. Estimating the data in Table 2, one has to keep in mind that the limit for thermostability and temperature control in our setup was  $\pm 0.003$  K and that the gate time of the counter was 1 s. We generally set the noise of the TSMR to 0.1 Hz, since we were not able to reach a better resolution in measuring all the devices simultaneously. Precise measurements, however, showed that, for 30 MHz TSMRs, it was about 0.03 Hz and for 10 MHz about 0.01 Hz under vapor stream and temperature control of the circuitry.

To reduce the noise, polymers leading to low noise (polymer nature) and low temperature sensitivity of the devices must be applied. In addition, enormous efforts must be made to even better thermostat the gas phase, the devices, and the circuitry. Extending the gate time of the counter is not reasonable with respect to practical applications.

A convenient scaling law for SAW delay lines has been that the noise levels can be approximated as 1 part in  $10^7$ .<sup>37</sup> For comparison, Zellers et al. recently reported 2 s RMS values of the baseline between 11 and 15 Hz for various 50–90 nm thick polymer films on 158 MHz SAW oscillators from Microsensor Systems Inc. (Bowling Green).<sup>38</sup> Grate and Klusty compared in an extensive study delay line and resonator structures of different fundamental frequencies.<sup>16</sup> They found best noise levels of 5–7 Hz for the 158 MHz delay lines (Microsensor Systems Inc.), and typical noise levels of 15–40 Hz for 400 MHz, 26–55 Hz for 300 MHz, and 3–10 Hz for 200 MHz resonators (Sawtek Inc., Orlando, FL) during vapor response experiments using poly(vinyltetradecanal) layers (250 kHz frequency shift due to coating).<sup>16</sup>

In the evaluation of our data, the limits of detection (LODs, S/N = 3) were determined experimentally and not by extrapolation of data obtained in measuring higher concentrations (see example in Figure 6). It has to be noted that it is very difficult to adjust low analyte concentrations in a flow apparatus of one dilution step using the common flow controllers (Tylan, Eching, Germany; 200, 100, 50, and 10 mL maximum flow) with a minimum adjustable flow of about 0.2 mL. Since all the devices have been measured simultaneously, the error in adjusting the concentrations is identical and affects only the absolute values but has no effect on the comparison. Checking the absolute analyte concentrations by GC measurements showed that there

(35) Kraus, G.; Gauglitz, G. *Fresenius J. Anal. Chem.* **1994**, 349, 399–402.

(36) Ricco, A. J., personal communication.

(37) Wohltjen, H. *Sens. Actuators* **1984**, 5, 307–325.

(38) Zellers, E. T.; Batterman, S.; Han, M.; Patrash, S. *Anal. Chem.* **1995**, 67, 1092–1106.



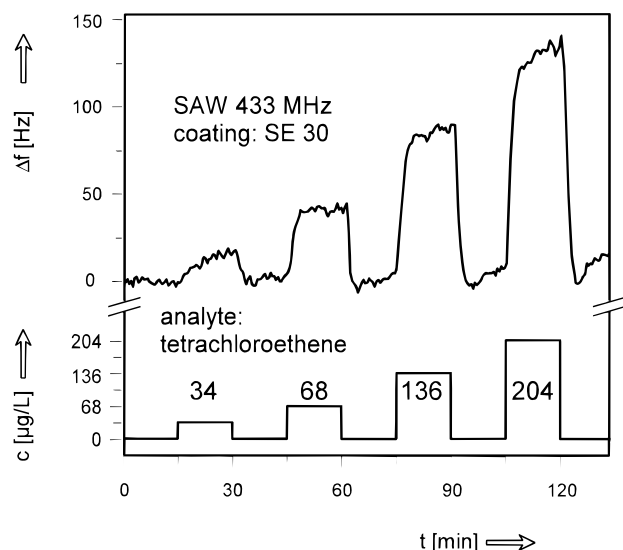


Figure 6. Typical responses of SE 30-coated 433 MHz SAW (exposure to tetrachloroethene).

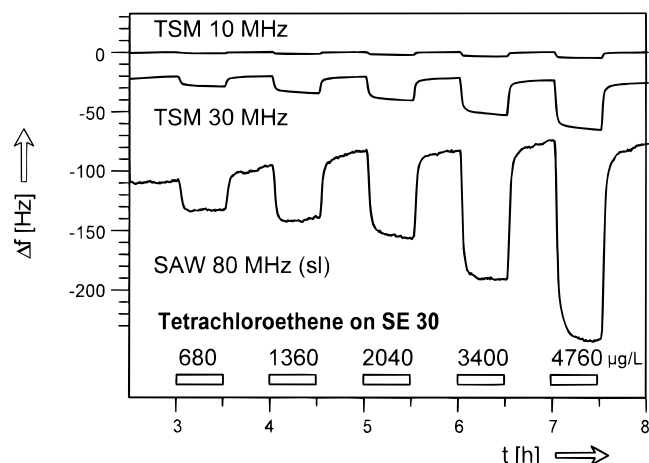


Figure 7. Comparison of response signals of 10 and 30 MHz TSMRs and an 80 MHz SAW coated with identically thick layers of SE 30 (analyte, tetrachloroethene).

may occur deviations up to 30% in this low concentration range. For measuring analyte concentrations below 5  $\mu\text{g/L}$  (1 ppm), it is necessary to dilute the analyte vapor in two steps down to the desired values.

An additional experiment involved applying the same polymer layer thickness to all the devices and evaluating the signals, signal/noise ratios, and partition coefficients. We chose 18 nm of SE 30 as a layer applicable to all the devices. The original signals for three of the devices are depicted in Figure 7. Since the signals of the 433 MHz device were by far higher, we list them only in Table 3.

The surface roughness of the employed AW quartz substrates determined by REM measurements was in the range of 50 up to 500 nm, depending on the polishing. Consequently, the application of an 18 nm film may lead to a nonclosed polymer surface, and it has to be noted as well that only one side of the TSM devices was coated. Coadsorption at the bare device and substrate/polymer interface may arise and hence significantly change the partition coefficient. As can be seen from Table 3, the partition coefficient was clearly enhanced, especially for the TSM devices coated on only one side and showing larger surface roughness. Mc Gill et al. reported for 50 nm films on 200 MHz

Table 3. Data for the Different Transducers Coated with Identically Thick Layers (18 nm of SE 30)<sup>a</sup>

device	$\Delta f_{\text{poly}}$ (kHz)	$\Delta f_{\text{gas}}$ (Hz)			S/N (3400 $\mu\text{g/L}$ )	$\log K$
		2040 $\mu\text{g/L}$	3400 $\mu\text{g/L}$	4760 $\mu\text{g/L}$		
10 MHz	0.47	2.6	3.9	5.2	52	3.30
30 MHz	4.2	18.6	28.7	39.0	390	3.37
80 MHz	13	64	95	128	160	3.35
433 MHz	404	1255	2025	2824	700	3.20

<sup>a</sup>  $\Delta f_{\text{poly}}$ , frequency shift due to coating;  $\Delta f_{\text{gas}}$ , sensor responses to 2040, 3400, and 4760  $\mu\text{g/L}$  tetrachloroethene; S/N, signal-to-noise ratio calculated for 3400  $\mu\text{g/L}$  (the TSMR noise was set to 0.1 Hz for all the calculations);  $\log K$ , logarithm of the respective partition coefficients.

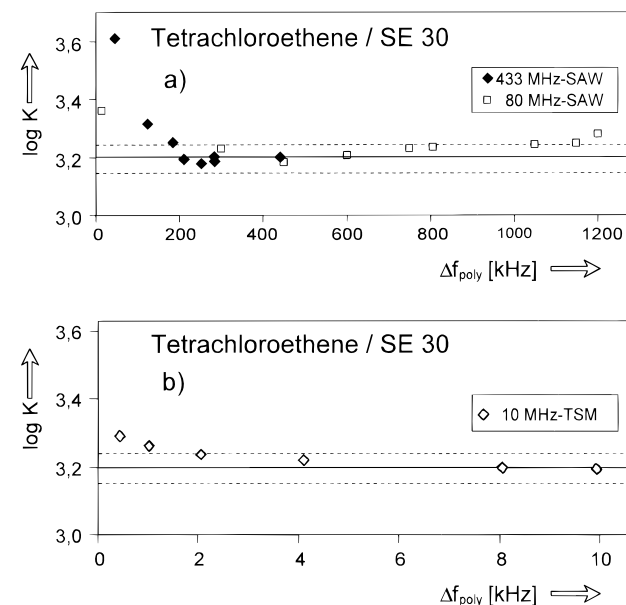


Figure 8. Logarithm of the partition coefficient ( $\log K$ ) versus layer thickness (represented by  $\Delta f_{\text{poly}}$ ) for different devices. The layer consisted of SE 30, and the analyte was tetrachloroethene. The dashed lines mark the range of  $\pm 10\%$ .

SAW devices significant contributions of interfacial and surface adsorption.<sup>39</sup> They attributed in some instances even the major components of the sensor responses to these effects.<sup>39</sup> In Figure 8, the effects of the layer thickness (represented by the frequency shift due to coating,  $\Delta f_{\text{poly}}$ ) on the partition coefficient are shown for a 10 MHz TSMR and 80 and 433 MHz SAWs. For all the devices under investigation, the tendencies were similar: too high partition coefficients at very thin layers (incomplete covering) and a broad range of layer thicknesses where the partition coefficient was stable within experimental error. In addition, it can be seen in Table 3 that, when applying very thin layers, the SAWs show better performance (S/N). However, it has to be noted that the noise assumed as 0.1 Hz for our TSMRs was somewhat lower.

In summary, the partition coefficients at low analyte concentrations were constant for the chosen analyte/polymer combination and independent of the type of transducer used. But it was crucial to select adequate polymers, to prepare closed polymer films that were thick enough to avoid coadsorption, to limit the maximum

(39) McGill, R. A.; Grate, J. W.; Anderson, M. In *Interfacial Design and Chemical Sensing*; Mallouk, T. E., Harrison, D. J., Eds.; ACS Symposium Series 561; American Chemical Society: Washington, DC, 1994; Chapter 24, pp 280–294.

film thickness for SAWs (plasticization, stiffness, etc.), and to apply only low analyte concentrations to operate in a range where Henry's law holds.

Evidently, the polymer SE 30 was particularly suitable for the direct comparison of transducer performances in our study. For PCPMS, problems arose in the direct comparison from its polarity and the low conductivity (0.05–0.01  $\mu\text{S}$  depending on the layer thickness), which limited the layer thickness of the SAW devices. Poly(ether urethane) was not universally applicable to 433 MHz since the sensor responses due to gas exposure (e.g., *n*-octane) showed a pronounced nonlinear behavior (thin and thicker layers) and increases in the device frequency which are attributable to changes in stiffness and plasticization.

Comparing all tested AW devices under gas exposure, the 30 MHz TSMRs showed very favorable S/N and LOD values.

## CONCLUSION

As can be seen from this head-to-head comparison and has been commonly held for a number of years,<sup>10</sup> the SAW devices offer the principal advantage of large response signals and enhanced surface sensitivity, which is particularly suitable if very thin layers (e.g., LB films, SAMs) are chosen. This holds for *molecular recognition occurring at or near the surface* and absorption in comparably thin, bulky polymer layers (see Table 3). The ability to take advantage of multiple transduction mechanisms makes the SAW a more versatile sensor platform than the TSM. Unambiguity of the sensor responses and the possibility to predict them, however, are only given if mass loading effects dominate. The thermosensitivity, the consequently observed noise of coated SAW devices, and the very strict high frequency requirements are important drawbacks. The experimental setup requires significant efforts and know-how concerning shielding, grounding, and temperature control. The limit for stabilizing the temperature in our setup was  $\pm 0.003$  K, as controlled by a thermoquartz. Considering the necessary efforts, it does not seem realistic for practical applications that better temperature stability can be achieved. The thermal fluctuations determine the lower limit for the frequency noise and hence the S/N and LOD values of the devices.

If, on the other hand, *molecular absorption occurs in the bulk*, as is the case for all polymers commonly used to monitor VOCs, the TSM devices are by far easier to handle, and the interpretation of the results (possibility to predict sensor responses) is more straightforward and simple since the TSMRs are mainly gravi-

metric detectors. Regarding the temperature drifts only, the 10 MHz TSMR is the most stable device, but the sensor responses are comparably low. In our studies, the 30 MHz TSM device appears to offer a good compromise concerning LOD, S/N, temperature behavior, and easy handling. Compared to SAW devices, it is much less sensitive to the small fluctuations in shear modulus that occur in the polymer with small temperature changes. Only simple high frequency requirements have to be met, and the device and circuitry are robust. It is possible to connect more than 100 m of coaxial cable between the sensor (miniaturized oscillating circuit included) and the recording unit.<sup>40</sup> In addition, problems arising in SAWs from the dynamics and viscoelastic properties of the polymer layer (described in refs 13, 14, 30, and 31) are small due to the lower operating frequency of the TSMRs. So, in summary, the TSMRs should not be forgotten as useful devices for immediate practical applications. This holds in particular for the field of environmental routine monitoring of organic volatiles with bulky polymer layers as chemically sensitive transducer coatings.

The selection of an AW technology and an appropriate coating must be made within the context of the application of interest. A very careful selection of the polymers is required, since noise levels, thermal effects, and consequently LOD values are strongly dependent on the polymer nature. In particular, it is clear that the respective polymer and the film thickness one chooses will greatly affect the limit of detection for each different device, not only due to the affinity of the polymer for the analyte but also perhaps even to a larger extent due to the effect on the device of changes in polymer viscoelastic properties (e.g., glass transitions) with temperature.<sup>36</sup> In addition, it is always necessary to calibrate each AW device, especially with respect to thermal effects, which mainly depend on the film morphology.

## ACKNOWLEDGMENT

We gratefully acknowledge Dr. Antonio J. Ricco (Sandia National Laboratories, Albuquerque, NM) for very helpful, detailed, and stimulating discussions and reading of the manuscript. We thank Dr. Michael J. Vellekoop (Xensor Integration, The Netherlands) for the donation of the Xensor setup and helpful remarks.

Received for review January 11, 1996. Accepted March 26, 1996.<sup>®</sup>

AC9600215

(40) Bodenhöfer, K. Diploma thesis, University of Tübingen, 1994.

<sup>®</sup> Abstract published in *Advance ACS Abstracts*, May 15, 1996.